TITLE: InAs Quantum Dots in AlAs/GaAs Short Period Superlattices: Structure, Optical Characteristics and Laser Diodes

Mat. Res. Soc. Symp. Proc. Vol. 692 © 2002 Materials Research Society H3.8

InAs quantum dots in AlAs/GaAs short period superlattices: structure, optical characteristics and laser diodes

Vadim Tokranov, M. Yakimov, A. Katsnelson, K. Dovidenko, R. Todt, and S. Oktyabrsky, UAlbany Institute for Materials, University at Albany–SUNY, 251 Fuller Rd, Albany, NY 12203

ABSTRACT

The influence of two monolayer - thick AlAs under- and overlayers on the formation and properties of self-assembled InAs quantum dots (QDs) has been studied using transmission electron microscopy (TEM) and photoluminescence (PL). Single sheets of InAs QDs were grown inside a 2ML/8ML AlAs/GaAs short-period superlattice with various combinations of under- and overlayers. It was found that 2.4ML InAs QDs with GaAs underlayer and 2ML AlAs overlayer exhibited the lowest QD surface density of $4.2x10^{10}$ cm^{-2} and the largest QD lateral size of about 19 nm as compared to the other combinations of cladding layers. This InAs QD ensemble has also shown the highest room temperature PL intensity with a peak at 1210 nm and the narrowest linewidth, 34 meV. Fabricated edge-emitting lasers using triple layers of InAs QDs with AlAs overlayer demonstrated 120 A/cm^2 threshold current density and 1230 nm emission wavelength at room temperature. Excited state QD lasers have shown high thermal stability of threshold current up to 130 °C.

INTRODUCTION

Quantum dot (QD) layers were proposed as an active gain medium for semiconductor laser diodes in 1982 [1]. After the discovery of self-assembly of QDs in the InAs/GaAs system via Stranski–Krastanov growth mode, significant research efforts were directed to obtain QD ensembles with uniform size, high density, and high emission efficiency [2,3], and to fabricate QD lasers [4,5,6]. Currently, the performance of QD lasers is comparable or even better than that of quantum well (QW) lasers, e.g. room temperature threshold current density of 16 A/cm^2 for single- and 36 A/cm^2 for triple-layer QD laser [6], and long wavelength (1.3 μm) lasing on GaAs substarte [5] were obtained. However, InAs/GaAs quantum-dot lasers with the lowest threshold current density (ground level near 1.3 μm emission wavelength) have not yet achieved high-temperature stability [7].

In spite of profound studies of Stranski–Krastanov growth of In(Ga)As islands on GaAs, this self-organized formation of nanoscale islands is still not completely understood. The structural and optical properties of QD ensembles are very sensitive to the growth parameters [8,9]. This phenomenon of self-assembly is further complicated by intermixing of InAs QDs with the GaAs barrier [10], segregation of In atoms when InGaAs islands are overgrown by GaAs [11,12], complex diffusion properties of adatoms. Very recently, the top Al containing layers have been used to achieve a red shift of the InAs QDs photoluminescence band [13,14].

The primary goal of the present study is the development of the self-assembled QD active medium for laser diodes operating at elevated (>100°C) temperatures. We have investigated the influence of two monolayer - thick AlAs under- and overlayers on the formation and properties of InAs QDs in a short period superlattice (SPSL) using transmission electron microscopy (TEM) and photoluminescence (PL).

EXPERIMENTAL DELAILS

The structures were grown on GaAs(100) substrates in EPI GEN II Molecular Beam Epitaxy (MBE) system equipped with As-valved cracker source. For QD growth, InAs growth rate was maintained at 0.048±0.002 ML/s, and As_2 flux was kept constant at $1.5x10^{-6}$ Torr. Indium flux was calibrated by InGaAs growth using reflection high energy electron diffraction oscillations. The self-assembled InAs QDs were embedded into 2ML-AlAs/8ML-GaAs SPSL barrier. The closest to the QDs four SPSL periods were grown at the QD growth temperature.

The PL and TEM measurements were carried out on the same samples with QD layers placed 30 nm below the surface. The growth was started with 500 nm of $Al_{0.45}Ga_{0.55}As$ cladding alloy followed by 280 nm SPSL grown at 650 °C. Then, the growth was interrupted to reduce the substrate temperature to that for QD growth (450 - 500 °C). InAs QDs were grown using different combinations of 2ML-AlAs and 8ML-GaAs underlayers and overlayers. The self-assembled QDs were then capped with four periods of SPSL, and after heating up the substrate by 80 °C, 3 periods of SPSL and 10 nm of AlGaAs alloy were grown on the top.

The optical properties of the self-assembled QDs were characterized using PL. The top and bottom $Al_{0.45}Ga_{0.55}As$ cladding layers were used to prevent photogenerated carriers from spreading to the substrate or to the surface. We used an Ar^+ ion laser (514.5nm) as an excitation source. The PL spectra were detected by LN_2-cooled Ge p-i-n photodiode and recorded using lock-in techniques.

The laser diode structures were grown on n-type GaAs(100) substrates. Si and Be were used for n–type and p–type doping, respectively. n^+–GaAs buffer layer and 1 μm - thick bottom n-$Al_{0.7}Ga_{0.3}As$ cladding layer were grown at 610°C. They were followed by an undoped 900 nm - thick SPSL waveguide structure with the QD active layers in the center. The bottom half of the SPSL waveguide and the QD layers were grown at 650 °C and 475 °C, respectively, following a similar temperature ramping procedure as for PL/TEM samples. Triple layers of InAs QDs with GaAs underlayer and AlAs overlayer, and 30 nm SPSL spacing were used as the laser active medium. Top half of the SPSL waveguide, 1 μm – thick p-$Al_{0.7}Ga_{0.3}As$ cladding layer and the top 250 nm - thick p^+-GaAs contact layer were all grown at 570°C to prevent thermal evolution of the QD structure. Gain-guided lasers with stripe width from 10 to 200 μm and cavity lengths from 1.5 to 10 mm were fabricated from these structures. Laser diodes were fabricated by cleaving without any coating of the facets. Stripe-up laser crystals were mounted on a heatsink using In solder.

RESULTS AND DISCUSSIONS

Transmission Electron Microscopy (TEM): QDs Imbedded into Short Period SL

To optimize the properties of QD structures for the laser gain medium, we have started with the investigation of the influence of GaAs and AlAs under- and overlayers and growth temperature on size, size distribution, surface density and PL properties of QDs. We have grown a set of samples at the substrate temperature in the range of 450 - 500 °C with 2.4ML of InAs imbedded into 8ML-GaAs/2ML-AlAs SPSL. Some of the advantages of SPSL are that this is an effective wide-bandgap material grown at relatively low temperature and another variable to control the emission wavelength. We have investigated four basic QD designs: (i) with 8ML GaAs as both under- and overlayer; (ii) the same but with 2ML AlAs; (iii) with 8ML GaAs

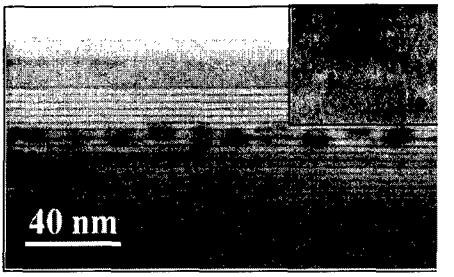

Fig. 1. Cross-sectional TEM image of QD array (2.4ML InAs with AlAs under- and overlayer). Inset: cross-sectional high-resolution TEM image of a single QD.

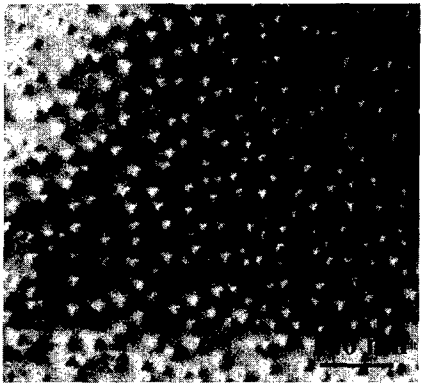

Fig. 2. TEM plan-view micrograph of QDs grown at 475 ^{0}C on AlAs with 2ML AlAs overlayer (small QDs ~14 nm).

underlayer and 2ML AlAs overlayer; and (iv) with 2ML AlAs underlayer and 8ML GaAs overlayer.

200 keV TEM (JEOL 2010 FEG) was used for plan-view and cross-sectional studies. Fig. 1 shows a cross-sectional TEM image of a single layer 2.4ML InAs QDs with 2ML AlAs on both sides imbedded into SPSL. The strain contrast originating from the QDs is clearly visible. One can also observe that the SPSL is an effective way for structure smoothening after the QD growth. The inset in the Fig. 1 shows a cross-sectional high-resolution TEM image of a single QD demonstrating its typical pyramidal shape.

Plan-view image of a QD ensemble grown at 475 °C with 2ML AlAs under- and overlayer is presented in Fig. 2. Statistical analysis of plan-view micrographs allowed us to evaluate the surface density and average size of quantum dots. In Fig. 3, we plot the QD surface number density as a function of the growth temperature. All the studied QD designs exhibit a reduction of surface density at higher substrate temperatures, but the samples with AlAs overlayer are less sensitive to this parameter. The highest QD density of about $2x10^{11}$ cm^{-2} was obtained in the structures with AlAs underlayer and GaAs overlayer. This results from the lower diffusion rate of In adatoms on the AlAs surface as we have observed recently [15].

On the contrary, QDs with GaAs underlayer and AlAs overlayer had the lowest surface density of about $3x10^{10}$ cm^{-2} at 500 °C. The average QD size dependance on the growth temperature is shown in Fig. 4 for various QD designs. Generally, QD sizes increase with the growth temperature, and QDs on GaAs with 2ML AlAs overlayer exhibit the largest sizes. In the case of AlAs overlayer (as compared to GaAs), we have observed an increase of the average size and reduction of the surface density likely because of dissolving of small QDs and wetting layer by AlAs overlayer [14]. GaAs underlayer instead of AlAs also leads to increased size and reduced density of QDs. In this case, it is due to the higher surface diffusion of In adatoms on GaAs surface [15]. The main result from these TEM studies is that InAs QDs grown at 475 °C on GaAs underlayer and capped with AlAs overlayer exhibit the lowest QD surface density of $4.2x10^{10}$ cm^{-2} and the largest QD lateral size of about 19 nm as compared to the other combinations of the cladding layers. This QD ensemble is expected to be very promising for manufacturing of the QD medium with low ground state energy near 1.3 μm and narrow size distribution. It should be noted, that the laser applications require high density and high optical

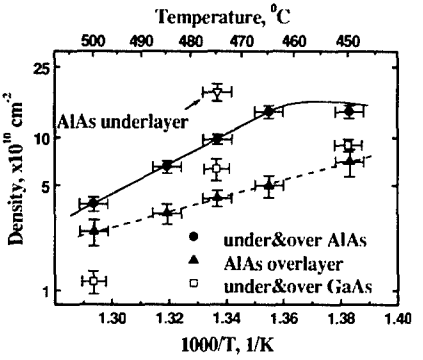

Fig. 3. Surface density of 2.4ML InAs QDs with different under- and overlayers as a function of growth temperature.

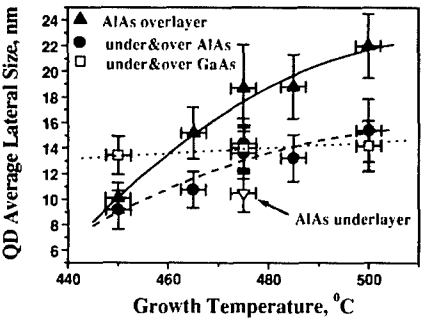

Fig. 4. Average sizes of 2.4ML InAs QDs with different under- and overlayers vs. growth temperature. Vertical error bars correspond to the QD size dispersion.

quality of the QD ensemble, which are usually quite conflicting demands. Next section is devoted to the optimization of the PL properties of the QDs.

Photoluminescence: optical properties of QDs imbedded into SPSL

Fig. 5 shows PL peak energy and FWHM of the luminescence band as a function of the average lateral size of QDs grown with different under- and overlayers at 475 °C . These data were obtained at room temperature with the excitation intensity of 10 W/cm^2. The PL band is found to shift towards the lower energies with increasing of QD sizes as expected from a simple quantum size effect. On the contrary, the effect of barrier bandgap is obscured by the size effect. For example, QDs capped with AlAs high-bandgap overlayers exhibit noticeable PL redshift in comparison with those overgrown by low-bandgap GaAs. Significant reduction of FWHM of the luminescence band indicates that the homogeneity of the QD sizes is also improved for large QDs. Therefore, our growth conditions with the increased In adatom diffusion length lead not only to the increase of the QD sizes, but also to the improved size distribution.

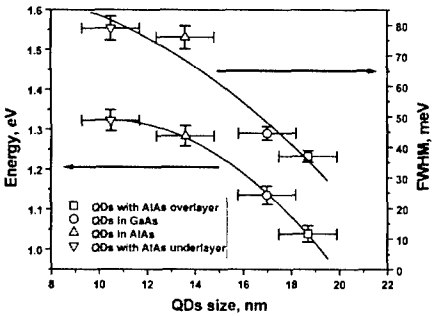

Fig. 5. Room temperature PL peak energy and band FWHM of 2.4ML InAs QDs as a function of average sizes of QD layers with different design.

QD ensemble with 2ML AlAs overlayer has demonstrated the highest room temperature PL intensity and the lowest band FWHM of 34 meV (at low excitation level, 0.1 W/cm^2) in comparison with the other QD designs. The highest room temperature PL intensity indicates the reduction of density of nonradiative recombination centers in the sample with the lowest QD surface concentration grown with AlAs overlayer.

Though the AlAs layers are usually expected to have higher defect density than GaAs, we have not observed any degradation of the QD radiative recombination associated with the presence of AlAs.

Electroluminescence of triple QD layer edge-emitting lasers

All electroluminescent (EL) measurements were carried out under pulsed excitation in a temperature range 77 - 430 K. The excitation pulse width was 1 μs with a duty cycle factor of about 0.5%. The EL spectra of an edge-emitting laser with a triple 2.2ML InAs QD layers operating on the ground state transitions are shown in Fig. 6. Light-current characteristic is plotted in the inset. Ground state lasing was obtained at a threshold current density, J_{th} = 120 A/cm^2, and wavelength, 1.23 μm. Minimum cavity length for the ground state lasing was found to be 6 mm. We have estimated the maximum modal gain of our structure, 3.5 cm^{-1}, assuming similar intrinsic losses (α_i=1.8 cm^{-1}) as in the case of quantum well heterolaser with the same waveguide width (0.9 μm). We expect that these results can be significantly improved by optimization of the laser heterostructure, especially by increasing of a potentially low optical confinement factor of the QD active medium.

The EL spectra of an edge-emitting laser with a triple 2.0ML InAs QD layers operating on excited state transitions are shown in Fig. 7, with a corresponding light-current characteristic plotted in the inset. In this case, the lasing was achieved at a higher current density, J_{th} = 360 A/cm^2, and shorter wavelength, 1.14 μm. Minimum cavity length for ground state lasing was about 3 mm, corresponding to the maximum modal gain of the excited state of about 5 cm^{-1} in our structure. These results can be also improved by at least 2-3 times by optimization of the laser heterostructure, such as decreasing the waveguide width down to 0.25 μm, decreasing intrinsic losses by 20-30% down to the best reported values, 1.3 - 1.5 cm^{-1} [6].

Thermal quenching of the laser threshold current is plotted in Fig.8. The maximum working temperature for the ground state laser was found to be 75 °C that corresponds to the currently reported values. Excited state lasers exhibited weaker temperature dependence of the threshold current with the maximum operating temperature exceeding 130 °C. The primary reason for the higher thermal stability of excited state QD lasers is the higher saturated modal gain [6]. An additional reason for poor thermal stability of the ground state QD lasers is the stress in a very long laser crystal mounted on a copper heatsink because of the difference in

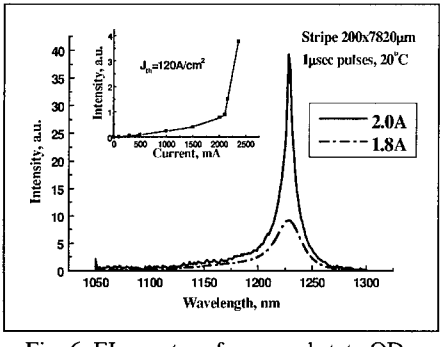

Fig. 6. EL spectra of a ground state QD laser. Inset: Ground state QD laser light-current characteristic.

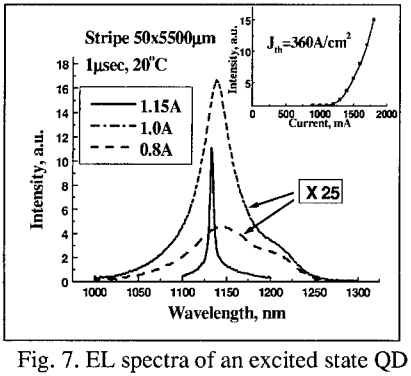

Fig. 7. EL spectra of an excited state QD laser. Inset: QD laser light-current characteristic.

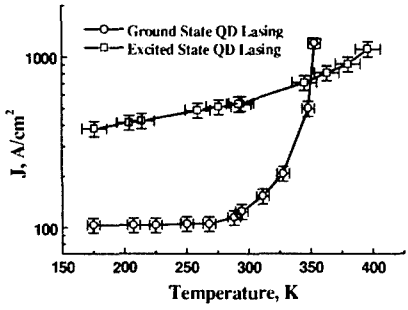

Fig. 8. Threshold current density dependence on temperature for ground state and excited state QD lasers.

thermal expansion coefficients of GaAs and copper. Therefore, synthesis of multilayered QD structures with high QD number density and low nonradiative recombination probability is still a challenging goal for low threshold QD lasers operating at high temperatures.

CONCLUSIONS

To accelerate optimization of QD growth technology and understanding of the growth mechanisms we have used QD structures suitable for both photoluminescent characterization and TEM plan-view measurements of QD density and average size. By employing of this combined method, we have found that 2.4ML InAs QDs with GaAs underlayer and 2ML AlAs overlayer exhibited the highest PL efficiency at room temperature, the narrowest band FWHM (34 meV), the lowest QD surface density of $4.2 \cdot 10^{10}$ cm^{-2} and the largest QD lateral size of about 19 nm, as compared to the other combinations of cladding layers. Edge-emitting laser with triple 2.2ML InAs QD layers operating at the ground state transitions demonstrated low room temperature threshold current density of 120 A/cm^2 and working temperature up to 75 °C. Excited state triple 2ML InAs laser showed threshold current density of 360A/cm^2, and high operation temperature up to 130 °C.

ACNOWLEDGMENTS

The work was supported by MARCO and DARPA under the National Focus Center for Interconnects for Gigascale Integration. This support is greatly appreciated.

REFERENCES

1. Y. Arakawa, and H. Sakaki, Appl. Phys. Lett., **40**, 939 (1982).
2. D. Leonard, M. Kishnamurthy, C. M. Reaves, et al., Appl. Phys. Lett., **63**, 3203 (1993).
3. N. N. Ledentsov, V. M. Ustinov, A. Yu. Egorov, et al., Semicond., **28**, 832 (1994).
4. D. Bimberg, N. N. Ledentsov, M. Grundmann, et al., Physica E., **3**, 129 (1998)
5. G. Park, D L. Huffaker, Z. Zou, et al., IEEE Photon. Technol. Lett., **11**, 301 (1999).
6. P. G. Eliseev, H. Li, A. Stintz, T. C. Newell, et al., Appl. Phys. Lett., **77**, 262 (2000).
7. X. Huang, A. Stintz, C. P. Hains, et al., IEEE Photon. Technol. Lett., **12**, 227 (2000).
8. L. Chu, M. Arzberger, G. Böhm, and G. Abstreiter, J. Appl. Phys., **85**, 2355 (1999).
9. S. Fafard, Z. R. Wasilewski, C. Ni. Allen, D. Picard, et al., Phys. Rev. B, **59**, 15368 (1999).
10. P. B. Joyce, T. J. Krzyzewski, G. R. Bell, et al., Phys. Rev. B., **58**, R15981 (1998).
11. O. Brandt, L. Tapfer, K. Ploog, R. Bierwolf, et al., Appl. Phys. Lett., **61**, 2814 (1992).
12. U. Woggon, W. Langbein, J. M. Hvam, et al., Appl. Phys. Lett., **71**, 377 (1997).
13. M. Arzberger, U. Käsberger, G. Böhm, et al., Appl. Phys. Lett., **75**, 3968 (1999).
14. A. F. Tsatsul'nikov, A. R. Kovsh, A. E. Zhukov, et al., J. Appl. Phys., **88**, 6272 (2000).
15. M. Yakimov, V. Tokranov, and S. Oktyabrsky, MRS Symp. Proc., **648**, P2.6.1 (2001).